Synthesis and Anticancer Activity of Brefeldin A Ester Derivatives

Nwanne O. Anadu, V. Jo Davisson, and Mark Cushman*

Department of Medicinal Chemistry and Molecular Pharmacology, School of Pharmacy and Pharmaceutical Sciences, and the Purdue Cancer Center, Purdue University, West Lafayette, Indiana 47907

Received March 13, 2006

Ester derivatives of brefeldin A (BFA) were synthesized to determine which of its two hydroxyl groups could be modified while still maintaining biological activity. The compounds were tested for antiproliferative activity in the National Cancer Institute's 60 cancer cell line screen. Monoderivatization at the C4 and C7 alcohols was tolerated, yielding biologically active compounds, whereas the analogues derivatized at both positions were the least active in the series. Molecular modeling of the analogues revealed that both the C4 and C7 derivatives were well tolerated at the interface between ARF1 and its guanine nucleotide exchange factor ARNO. The Golgi-disruptive properties of the analogues were determined using fluorescence imaging assays. The BFA ester conjugates synthesized in this study were cytotoxic to cancer cells, and we have shown that the disruption of the Golgi complex is not necessary for cytotoxicity. The brefeldin A ester derivatives are potential anticancer agents.

Introduction

Brefeldin A (BFA[a]) (**1**) is a macrolide antibiotic that was first isolated from *Penicillium decumbens*.[1] It has a wide variety of biological properties, including antitumor, antiviral, antifungal, and antimitotic effects.[2−5] The in vitro mean graph midpoint (MGM) GI50 value of 40 nM for BFA was determined in the National Cancer Institute's 60 cancer cell line assay (NCI-60). Despite its potential to be a cancer chemotherapeutic agent, BFA faces some major limitations because of its poor solubility in biological fluids, undesirable pharmacokinetic properties, and neurotoxicity in animal studies.[6] Therefore, a need exists to synthesize BFA analogues that maintain potency yet have improved therapeutic properties and are less toxic. The lack of a clear understanding of BFA's mechanism of action limits its usefulness as a lead compound for anticancer drug development.

BFA administration has been associated with a novel disruption of the Golgi complex.[7] The reversible disassembly of the Golgi results in an interruption of protein transport and causes Golgi proteins to redistribute to the endoplasmic reticulum.[7−10] ADP ribosylation factors (ARFs) are a family of G-proteins involved in vesicle transport, Golgi maintenance, and signal transduction.[8−16] They cycle between GDP- and GTP-bound states that render them inactive or active, respectively. This nucleotide exchange is catalyzed by guanine nucleotide exchange factors (GEFs). In 2000, Robineau et al. discovered that BFA does not bind to ARF or its GEF protein in isolation but that it acts as an uncompetitive inhibitor that binds to a ternary complex of ARF−GDP−GEF, stabilizing this otherwise transient protein−protein interaction.[17] Protein crystal structures show BFA fitting in the hydrophobic pocket created in the interface between the ARF and GEF proteins.[18−22]

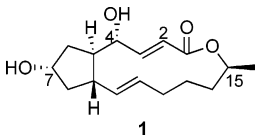

1

Figure 1. Brefeldin A

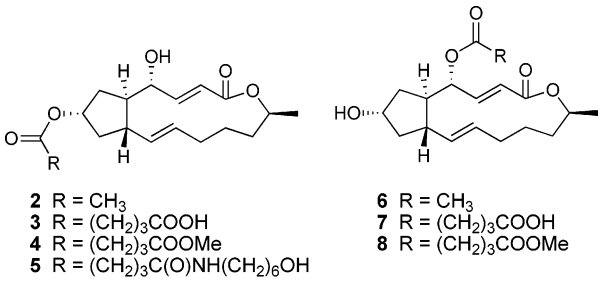

2 R = CH_3
3 R = $(CH_2)_3COOH$
4 R = $(CH_2)_3COOMe$
5 R = $(CH_2)_3C(O)NH(CH_2)_6OH$

6 R = CH_3
7 R = $(CH_2)_3COOH$
8 R = $(CH_2)_3COOMe$

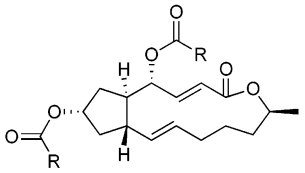

9 R = CH_3
10 R = $(CH_2)_3COOH$
11 R = $(CH_2)_3COOMe$
12 R = $(CH_2)_3C(O)NH(CH_2)_6OH$

Figure 2. Synthesized ester analogues of brefeldin A.

Recent discoveries have indicated that BFA-induced apoptosis is not dependent on the disassembly of the Golgi complex. The drug forskolin protected normal rat kidney cells from BFA-induced Golgi disruption and blocked BFA's ability to inhibit protein secretion.[23] However, in HCT 116 human colon cancer cells, BFA still induced apoptosis in the presence of forskolin, even though the same antagonistic Golgi effect was still observed.[24] This suggests multiple mechanisms of action for BFA and points to the existence of non-Golgi related targets. The synthesis of BFA derivatives may facilitate the exploration of different mechanisms of action and may lead to analogues with better selectivity.

* To whom correspondence should be addressed. Tel: 765-494-1465. Fax: 765-494-6790. E-mail: cushman@pharmacy.purdue.edu.

[a] Abbreviations: ARF, ADP ribosylation factor; BFA, brefeldin A; BSA, bovine serum albumin; EDCI, 1-[3-(dimethylamino)propyl]-3-ethylcarbodiimide hydrochloride; GDP, guanosine diphosphate; GEF, guanine nucleotide exchange factor; GSH, glutathione; GST, glutathione *S*-transferase; GTP, guanosine triphosphate; MGM, mean graph midpoint; MMFF, Merck molecular force field; MTT, 3-(4,5-dimethylthiazolyl-2)-2,5-diphenyltetrazolium bromide; NBD, *N*-[7-(4-nitrobenzo-2-oxa-1,3-diazole)]-6-aminocaproyl-D-erythro-sphingosine; NHS, *N*-hydroxysuccinimidyl; PDB, protein data bank; TBAF, *tert*-butylammonium fluoride; TBS, *tert*-butyldimethylsilyl group; TEA, triethylamine; THF, tetrahydrofuran.

10.1021/jm0602817 CCC: $33.50
Published on Web 06/01/2006

Scheme 1. Silylation and Selective Desilylation of BFA[a]

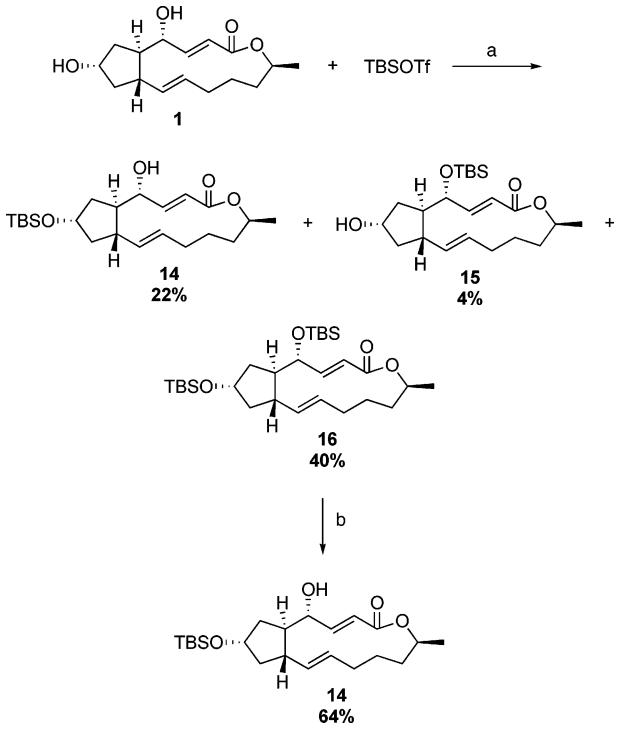

[a] Reagents (a) TBSOTf, 2,6-lutidine, CH_2Cl_2, 0−25 °C, 8 h; (b) TBAF, THF, 0−25 °C, 25 h.

The existing information on BFA structure−activity relationships indicates the requirement of the α,β-unsaturated lactone, the alkenes, and the conformational rigidity of the molecule for biological activity.[25,26] The C4 and C7 epimers of BFA were found to be inactive compared to the parent compound.[25−28] Methylation and oxidation of the C4 and C7 alcohols also resulted in reduced biological activity.[25,27,29,30] However, sulfide and sulfoxide prodrugs of BFA, which have increased aqueous solubilities, have shown promising antitumor effects in vitro and in vivo.[2,3] These compounds were obtained by the Michael addition of thiols to the α,β-unsaturated bond of BFA and are effective against cancer cells because they are soluble prodrugs that are designed to yield an intact BFA pharmacophore after drug metabolism.

The present article outlines the synthesis of mono and diester derivatives of BFA, which were obtained by modifying the two alcohols (at C4 and C7). The cytotoxicities of the C4 versus C7 mono and diester derivatives were determined in the NCI's 60 cell line screen. In principle, these compounds could act as drugs in their own right or as prodrugs of BFA that would be activated by cellular esterases. Esters with various chain lengths were synthesized to examine the steric tolerances of the binding site and to determine if longer chains could be considered for making brefeldin A bioconjugates and affinity columns.

Results and Discussion

Design and Synthesis. The synthesis of the monoesters was designed to exploit the difference in reactivity of the C4 and C7 alcohols. The C4 secondary allylic alcohol of BFA is in a sterically more hindered environment and is less reactive than the C7 alcohol. To synthesize the 4-ester derivatives, the 7-OH had to first be protected with a *tert*-butyldimethylsilyl (TBS) group using *tert*-butyldimethylsilyl triflate and 2,6-lutidine in dichloromethane (Scheme 1).[31] After esterification of the 4-hydroxyl, the 7-TBS group was removed by the reaction with *tert*-butylammonium fluoride in THF to yield the C4-ester derivatives.[32]

Scheme 2. Synthesis of C7 BFA Ester Derivatives[a]

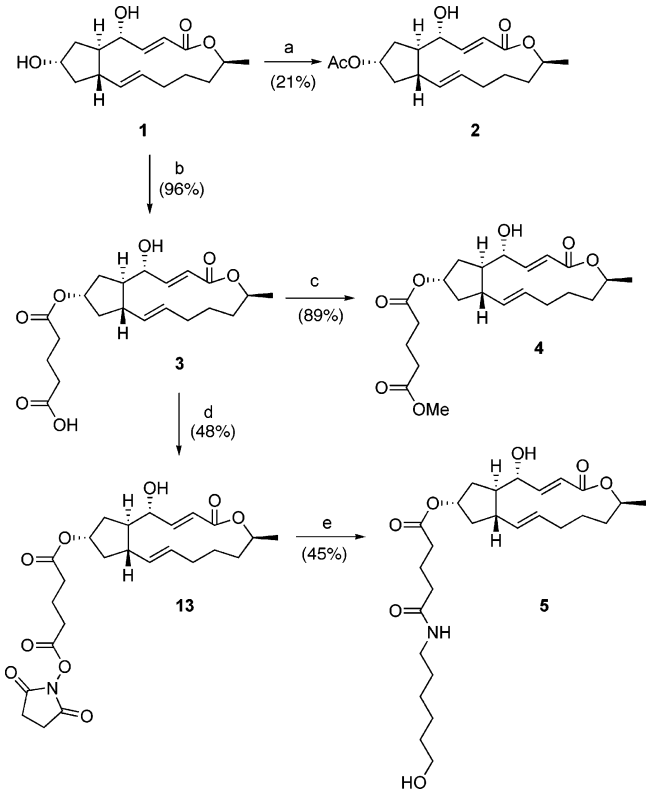

[a] Reagents (a) Ac_2O, 2,6-lutidine, 110 °C, 36 h; (b) glutaric anhydride, 2,6-lutidine, 110 °C, 12 h; (c) $TMSCH_2N_2$, MeOH, hexane, rt, 48 h; (d) *N*,*N*′-disuccinimidyl carbonate, DMF, 2,6-lutidine, 60 °C, 48 h; (e) 6-aminohexanol, DMF, TEA, rt, 16 h.

Acetates **2**, **6**, and **9** were included in this study to confirm the findings by Zhu et al. that substitutions at these positions could still result in the retention of biological activity. These acetates were prepared by reacting BFA with acetic anhydride in 2,6-lutidine.[25,26] Glutarates **3**, **7**, and **10** with polar carboxyl groups in the side chain were designed to increase the aqueous solubility and to provide functionality for further chain extension. These derivatives were prepared by reacting BFA with glutaric anhydride in 2,6-lutidine (Schemes 2−4).[3] Methyl glutarates **4**, **8**, and **11** were synthesized to promote drug delivery by presenting a less polar prodrug than the carboxylate that would pass more readily through membranes before intracellular hydrolysis. The methyl glutarates were obtained via two different methods. Monoesters **4** and **8** were made by reacting the glutarates with TMS-diazomethane, which methylates the carboxylic acid and not the free alcohol (Schemes 2 and 3).[33] Diester **11** was prepared by reacting BFA with methyl 5-chloro-5-oxo-valerate (Scheme 4).[34] Compounds **5** and **12** were designed to probe the linker chain length, which could be attached to the BFA pharmacophore for preparation of bioconjugates and affinity columns while maintaining biological activity and protein-binding affinity. Reacting the *N*-hydroxysuccinimidyl (NHS) ester **13** of BFA with 6-aminohexanol (Scheme 2) afforded the 7-glutarylamidohexanol derivative of BFA **5**.[35] Di(glutarylamidohexanol) derivative **12** was synthesized by reacting BFA 4,7-*O*-diglutarate **10** with 1-[3-(dimethylamino)propyl]-3-ethylcarbodiimide hydrochloride (EDCI) and 6-aminohexanol (Scheme 4).

Cytotoxicity in Cancer Cell Cultures. The BFA derivatives were tested for cytotoxicity in the NCI's 60 cancer cell line

Scheme 3. Synthesis of C4 BFA Ester Derivatives[a]

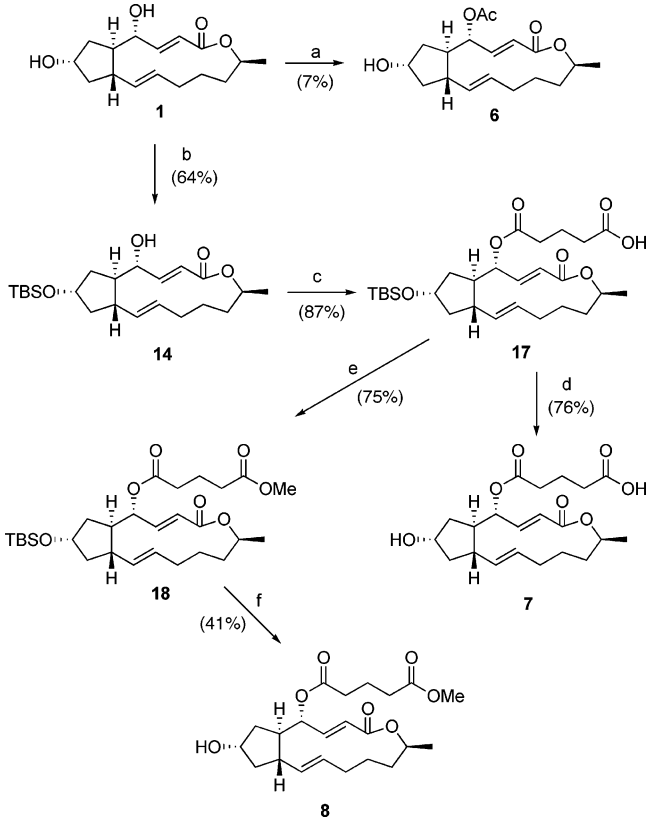

[a] Reagents: (a) Ac_2O, 2,6-lutidine, 110 °C, 36 h; (b) TBSOTf, 2,6-lutidine, CH_2Cl_2, 0−25 °C, 12 h; (c) glutaric anhydride, 2,6-lutidine, 110 °C, 12 h; (d) TBAF, THF, 0−25 °C, 25 h; (e) $TMSCH_2N_2$, MeOH, hexane, rt, 48 h; (f) TBAF, THF, 0−25 °C, 25 h.

Scheme 4. Synthesis of C4 and C7 BFA Diester Derivatives[a]

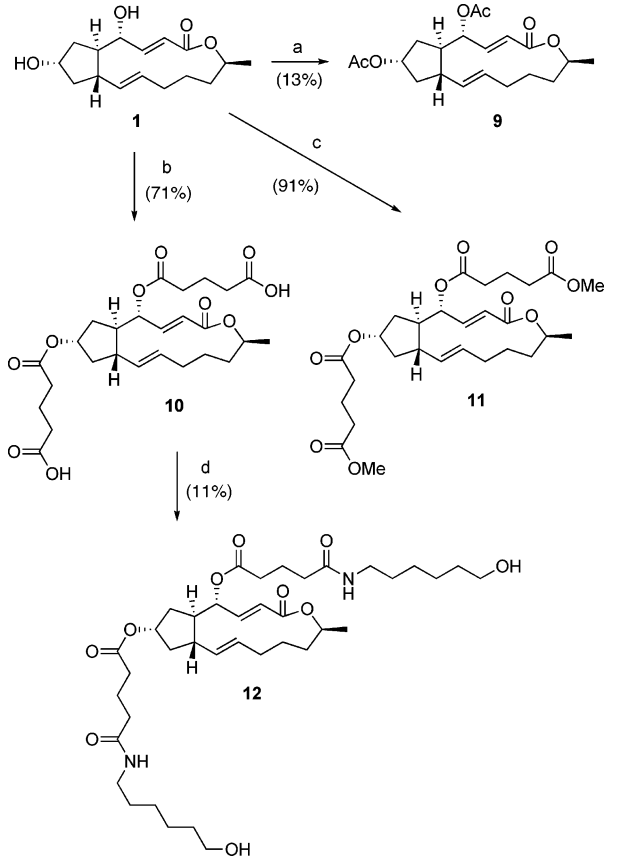

[a] Reagents (a) Ac_2O, 2,6-lutidine, 110 °C, 36 h; (b) glutaric anhydride, DMAP, 2,6-lutidine, 110 °C, 24 h; (c) methyl-5-chloro-5-oxovalerate, TEA, DMAP, CH_2Cl_2, 0 °C, 48 h; (d) EDCI, TEA, 6-aminohexanol, rt, 4 h.

screen. The procedure for the cytotoxicity assay is described in detail at the Developmental Therapeutics Program's website (http://dtp.nci.nih.gov/branches/btb/ivclsp.html). Briefly, the cancer cells are incubated with varying drug concentrations for 48 h, after which the cell viability was determined using a sulforhodamine B dye. The dose−response curves are generated from the cell viability data.

The mean graph midpoint (MGM) GI50 values are listed in Table 1. The MGM is based on a calculation of the average GI50 values for all of the cell lines tested (approximately 55) in which the GI50 values below and above the test range (10^{-8} to 10^{-4} M) are taken as the minimum (10^{-8} M) and maximum (10^{-4} M) drug concentrations used in the screening test. Therefore, the MGM value represents an overall assessment of the toxicity of the compound across numerous cell lines. Ester derivatives **2**, **4**, **5**, **8**, and **9** were able to maintain submicromolar MGM values, although none are more cytotoxic than BFA. The C4 and C7 analogues are equally active, whereas the diderivatized esters were the least active compounds. Table 1 shows representative data from the NCI-60 cancer cell line panel.

The methyl glutarates are more cytotoxic than their acid counterparts. BFA 7-*O*-methyl glutarate **4** with an MGM GI50 of 0.11 μM is 120-fold more potent than BFA 7-*O*-glutarate **3** (13.00 μM). A similar trend is seen with the C4 derivatives, where BFA 4-*O*-methyl glutarate **8** has an MGM GI50 of 0.16 μM compared to that of BFA 4-*O*-glutarate **7** (29.51 μM). This may be due to the fact that as charged species the glutarates are not able to cross the cell membrane, whereas the methyl glutarates are uncharged. The C7 acetate **2** mirrors BFA toxicity most closely, suggesting that it may possibly act as a prodrug that releases BFA upon activation by cellular esterases.

A close inspection of all 60 cell lines reveals that some analogues demonstrated better selectivity for certain cell lines. For example, BFA 7-*O*-methyl glutarate **4** had a GI50 of 0.05 μM in A549 (lung cancer cell line), whereas BFA 4-*O*-methyl glutarate **8** had a GI50 of 4.17 μM. Conversely, compound **4** had a GI50 of 0.20 μM in SN12C (renal cancer cell line) compared to 0.01 μM for compound **8** in the same cell line. In other cell lines such as PC3 (prostate cancer cells), compounds **4** and **8** are equally active. The reason for this selectivity has not yet been determined.

Chain-extended derivative **5** was submitted to the NCI for cytotoxicity testing, but given the long delay in response, the compound was subsequently submitted to the Purdue University Cancer Center as an alternative. It was tested in four available cell lines representing lung, colon, breast, and prostate cancers. The procedure used at the Purdue University Cancer Center is similar to that used by the NCI, but the cells are incubated with the drug for 72 h instead of 48 h, and therefore, the results are not directly comparable. The cell viability is determined using 3-(4,5-dimethylthiazolyl-2)-2,5-diphenyltetrazolium bromide (MTT) dye.

Metabolic Stabilities of BFA Ester Derivatives. The metabolic stabilities of **2**, **3**, and **4** in rat blood plasma were probed to determine if a correlation exists between the stability of the analogues toward esterases and the observed cytotoxicity. This study allowed us to determine the metabolic rates at which these compounds were converted to BFA and to predict the stability of solid-supported BFA in cell-free biological systems. The results from our analysis are given in Table 2. Acetate **2** has a half-life of 30 min in rat plasma, converting back to BFA.

Table 1. Cytotoxicities of BFA Ester Analogues[a]

	Cytotoxicity								
compd	lung	colon	CNS	melanoma	ovarian	renal	prostate	breast	MGM[b]
	A549	HCT-116	SF-539	UACC-62	OVCAR-3	SN12C	PC3	MCF7	GI50 (μM)
1	0.04	0.03	0.04	0.02	0.03	0.09	0.05	0.02	0.04 ± 0.019[c]
2	0.01	1.15	5.25	0.01	0.01	0.01	0.04	0.02	0.04 ± 0.004
3	33.20	21.38	22.39	NT[d]	20.42	32.36	19.50	19.05	13.00
4	0.05	0.04	0.07	0.13	0.03	0.20	0.06	0.04	0.11 ± 0.003
5[e]	0.70	0.65	NT	NT	NT	NT	0.33	0.18	0.47 ± 0.001
7	33.11	25.70	31.62	31.62	36.31	30.20	43.65	39.81	29.51
8	4.17	3.47	3.39	0.01	2.40	0.01	0.04	0.31	0.16 ± 0.002
9	0.85	22.91	58.88	0.01	1.48	0.01	2.14	2.63	0.45 ± 0.004
10	>100.00	>100.00	>100.00	>100.00	>100.00	>100.00	>100.00	>100.00	97.72
11	12.88	3.47	5.01	4.47	0.60	3.02	5.01	2.57	5.10

[a] The cytotoxicity GI50 values expressed in μM are the concentrations corresponding to 50% growth inhibition. [b] The mean graph midpoint for growth inhibition of all human cancer cell lines successfully tested. [c] The average of two experiments. [d] Not tested in this cell line. [e] This analogue was tested at the Purdue University Cancer Center on the four cell lines indicated.

Table 2. Metabolic Stabilities of BFA Esters[a]

compd	name	$t_{1/2}$
1	BFA	>24 h
2	BFA 7-*O*-acetate	30 min ± 1.2
3	BFA 7-*O*-glutarate	>24 h
4	BFA 7-*O*-methyl glutarate	3 min ± 0.35

[a] The reported half-lives are the average of three experiments.

The methyl glutarate **4** derivative was readily hydrolyzed to glutarate **3** in 3 min. However, glutarate **3** did not show evidence of hydrolysis to the parent BFA, even after 24 h. Glutarate compound **3** is not as easily hydrolyzed as the acetate, probably because of the fact that glutarate **3** is a free acid and is, therefore, tightly bound to plasma proteins. Because rat plasma esterases are more abundant and active than human esterases, it is likely that these analogues would be more stable to hydrolysis in humans. In an earlier in vivo pharmacokinetic study, it was found that BFA is cleared from rat plasma with a mean residence time of 11.5 min.[36,37] BFA was stable in our in vitro rat plasma assay, with no detectable metabolism occurring after 24 h. The rapid clearance in vivo is probably due to detoxification by glutathione *S*-transferase (GST). In Chinese hamster ovary cells, BFA bound to GSH via the Michael addition of the thiol to the α,β-unsaturated lactone of BFA, and the glutathione and cysteine conjugates were secreted into the medium.[38] Our results suggest that the glutarate-based BFA derivatives could have longer residence times than BFA in vivo.

Molecular Modeling. A crystal structure of BFA in the interface between ARF1-GDP and its GEF protein ARNO was recently published by Renault et al. (PDB code 1R8Q).[18] The position of BFA at the interface between the two proteins prevents the glutamic finger (GLU156) on the GEF protein from approaching the nucleotide on the ARF protein. This effectively traps the proteins in an abortive complex. In the absence of BFA, the proximity of the glutamic finger to the nucleotide results in unfavorable energetic conditions that cause the dissociation of the nucleotide. The analogues were modeled into this site to determine how well they would be tolerated in the interface and whether they would fulfill the binding interactions necessary for inhibiting the nucleotide exchange. The molecular models are shown in Figure 3. The positions of GLU156 (the glutamic finger), TYR190, and TRP78 are labeled. The latter two residues participate in hydrogen bonding with the C7 hydroxyl and are important for conferring sensitivity to BFA.[18]

The structure of BFA 7-*O*-methyl glutarate (**4**) was created in Sybyl v. 7.0 (Tripos, St. Louis, MO) and energy minimized using the Tripos force field and Gasteiger−Hückel charges.

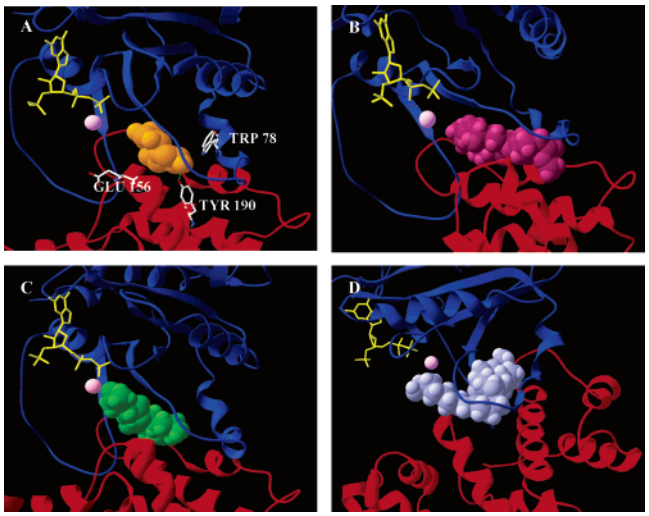

Figure 3. (A) Crystal structure of BFA in the ARF1−GDP−GEF interface. (B) Model of BFA 7-*O*-methyl glutarate (**4**) in the ARF1−GDP−GEF interface. (C) Model of BFA 4-*O*-methyl glutarate (**8**) in the ARF1−GDP−GEF interface. (D) Model of BFA 7-*O*-glutaryl-amidohexanol (**5**) in the ARF1−GDP−GEF interface. BFA, orange; BFA 7-*O*-methyl glutarate, purple; BFA 4-*O*-methyl glutarate, green; BFA 7-*O*-glutarylamidohexanol, light blue; guanosine-3′-monophosphate-5′-diphosphate, yellow; Mg^{2+} ion, pink; GLU156, green; ARF1, blue; GEF, red. Energy minimizations were done using Sybyl 7.0 (Tripos Inc., St. Louis, MO), and the images were viewed using the SwissPDB viewer (Geneva, Switzerland).

Compound **4** was modeled into the binding pocket between ARF and ARNO, overlapping with the structure of BFA, which was then deleted. The new complex was minimized with the MMFF94s force field and MMFF94 charges. The structures of the analogue, proteins, and the nucleotide were allowed to move during minimization. Chain-extended analogue BFA 7-*O*-glutarylamidohexanol (**5**) was also well tolerated in this active site, as shown in Figure 3. BFA 4-*O*-methyl glutarate (**8**) was also modeled into this site and is tolerated, showing coordination between the metal (Mg^{2+}) and the carbonyl oxygen on the chain.

Golgi Disruption Effects. Fluorescence imaging experiments were carried out to determine the effects that BFA (**1**), methyl glutarate analogues **4** and **8**, and diglutarate analogue **10** have on the Golgi complex. HCT116 cells were grown to 60−70% confluency and treated with 0.3 μM BFA or with the analogues for 30 min at 37 °C. This drug concentration exceeds the MGM GI50 values of **1**, **4**, and **8** but not **10**, as listed in Table 1. The cells were stained with a Golgi-specific dye, *N*-[7-(4-nitrobenzo-2-oxa-1,3-diazole)]-6-aminocaproyl-D-erythro-sphingosine (NBD

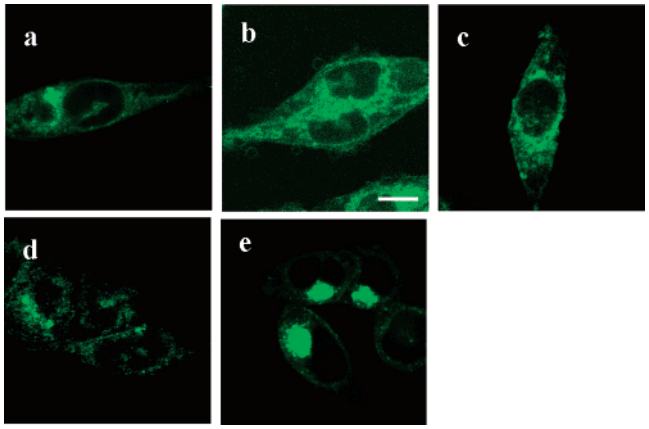

Figure 4. Golgi images of drug-treated HCT116 cells using NBD ceramide, a Golgi-specific fluorescent marker. (a) Untreated HCT116 cells; (b) 300 nM BFA-treated cells; (c) 300 nM BFA 7-*O*-methyl glutarate (**4**)-treated cells; (d) 300 nM BFA 4-*O*-methyl glutarate (**8**)-treated cells; and (e) 300 nM BFA 4,7-*O*-diglutarate (**10**)-treated cells. In all cases, the cells were treated with the drugs for 30 min. The bar indicates 10 μm.

ceramide), after drug incubation and visualized by confocal microscopy using the Bio-Rad MRC1024 inverted microscope at the Purdue University Cytometry Lab. The images in Figure 4 show the disruption of the Golgi complex by BFA and the analogues that were tested. The untreated cells in Figure 4a show the Golgi complex in distinct compact areas, whereas the BFA-treated cells show a more diffused staining of the Golgi. BFA 7-*O*-methylglutarate (**4**)-treated cells also show diffused staining but not as pronounced as that in cells exposed to BFA itself. BFA 4-*O*-methylglutarate (**8**)-treated cells show very weak disruption of the Golgi complex, and the cells treated with BFA 4,7-*O*-diglutarate (**10**) demonstrated the weakest effect. The results from the BFA 4-*O*-methylglutarate (**8**)-treated cells are most surprising, given the fact that the observed cytotoxicity is not significantly different from that of BFA 7-*O*-methylglutarate (**4**) (Table 1). The C4 compound **8** appears to disengage the mechanism of Golgi disruption from the antiproliferative activity.

Conclusions. The C4 and C7 ester derivatives of BFA were synthesized and analyzed for biological activity. The diderivatized compounds were the least active, perhaps because of their steric bulk in the binding site(s). Overall, the least potent analogues were the glutaric acid derivatives, probably because of their inability to efficiently cross the cell membrane as a result of their charged states. This problem was overcome by the methyl esters, which exhibited higher cytotoxicity in cancer cells. The methyl esters were readily hydrolyzed to the acids by rat plasma esterases in vitro. The molecular models indicate that the C4 and C7 derivatives are well tolerated in the interface between the ARF and ARNO proteins; however, the microscopy experiments showed that the C4 analogues were not as effective in disrupting the Golgi complex. However, the similarities in the cytotoxicities of the C4 and C7 series of compounds suggest the possibility of other binding sites for these analogues. The C4 compounds appear to uncouple BFA's Golgi disruptive activity from its cytotoxicity in cancer cells.

On the basis of the results obtained from molecular modeling, observed cytotoxicities, Golgi disruptive properties, and chemical syntheses, it may be concluded that the C7 position would be an ideal handle for the synthesis of BFA bioconjugates and affinity columns. Most importantly, these analogues display the potential for developing disease-specific agents. It is likely that multiple modes of action are possible with this class of compounds.

Experimental Section

^{1}H and ^{13}C NMR spectra were obtained using an ARX300 300 MHz Bruker NMR spectrometer, and where indicated, a DRX500 500 MHz Bruker NMR spectrometer was used. IR spectra were recorded on a Perkin-Elmer FTIR Spectrum One spectrometer. Column chromatography was performed with 230−400 mesh silica gel. Thin-layer chromatography was carried out using Aldrich silica gel polyester plates of 0.20 mm thickness and visualized with phosphomolybdic acid stain.

Brefeldin A 7-*O*-Acetate (2). BFA (0.10 g, 0.36 mmol) was dissolved in 2,6-lutidine (5 mL) at 110 °C. Acetic anhydride (0.02 mL, 0.30 mmol) was added dropwise over 2 h. The reaction mixture was allowed to stir at 110 °C for 36 h before the reaction was quenched by the addition of water (15 mL). Chloroform (2 × 15 mL) was used to wash the aqueous solution. The organic layer was rinsed with 1 M HCl (10 mL) and brine (15 mL) and dried over sodium sulfate. Compound **2** was purified from the crude product by flash chromatography on silica gel using a gradient eluant of 100% hexanes to 1:1 hexanes−ethyl acetate. The product was a thick clear oil (0.025 g, 21%). IR (thin film) 3468, 3019, 2400, 1708, 1216, 757 cm^{-1}; ^{1}H NMR ($CDCl_3$, 500 MHz) δ 7.33 (d, J = 15.77 Hz, 1 H) 5.90 (d, J = 15.69 Hz, 1 H), 5.70 (m, 1 H), 5.20 (m, 1 H), 5.15 (m, 1 H), 4.83 (m, 1 H), 4.10 (d, J = 9.22 Hz, 1 H), 2.35 (m, 1 H), 2.25 (m, 1 H), 2.17 (m, 1 H), 2.00 (s, 3 H), 1.84 (m, 2 H), 1.60−1.75 (m, 2 H), 1.50−1.60 (m, 4 H), 1.25 (d, J = 6.29 Hz, 3 H). 0.88−0.95 (m, 2 H); ^{13}C NMR ($CDCl_3$, 500 MHz) δ 170.1, 166.2, 151.0, 135.9, 117.2, 76.2, 75.1, 51.0, 43.6, 40.4, 38.0, 36.1, 33.7, 31.8, 21.4, 20.5; EIMS m/z 322 (M^+); analytical LC: column, Adsorbosphere HS C18; column dimensions, 250 mm × 4.6 mm; mobile phase, 1:1 CH_3CN:H_2O, 1 mL/min flow rate, RT = 10.92 min, 210−240 nm.

Brefeldin A 7-*O*-Glutarate (3). Brefeldin A (0.10 g, 0.36 mmol) was added to a round-bottomed flask containing freshly distilled 2,6-lutidine (3 mL). Glutaric anhydride (0.12 g, 1.1 mmol) was added to the solution. The mixture was allowed to stir at 110 °C for 12 h. The progress of the reaction was monitored by silica gel TLC using 7:3 ethyl acetate−hexanes with 1% acetic acid. After 12 h, the reaction was quenched with water (10 mL), and the mixture was extracted with dichloromethane (10 mL). The organic layer was washed with 1 M HCl (5 mL) and dried over sodium sulfate. Compound **3** was isolated as a yellow oil (0.135 g, 96%). IR (thin film) 3468, 2932, 1732, 1258 cm^{-1}; ^{1}H NMR ($CDCl_3$, 300 MHz) δ 7.30 (dd, J = 3.13 and 15.70 Hz, 1 H), 5.90 (dd, J = 1.94 and 15.70 Hz, 1 H), 5.70 (m, 1 H), 5.15 (m, 1 H), 4.80 (m, 1 H), 4.10 (m, 1 H), 2.10−2.40 (m, 9 H), 1.40−2.10 (m, 19 H), 1.25 (d, J = 6.21 Hz, 3 H), 0.90 (m, 1 H); ^{13}C NMR ($CDCl_3$, 300 MHz) δ 172.4, 166.6, 136.5, 131.3, 76.2, 75.9, 72.1, 52.7, 44.3, 33.2, 30.3, 27.1, 26.0, 21.2, 20.2; ESIMS m/z 417 (Na^+ adduct); analytical LC: column, Adsorbosphere HS C18; column dimensions, 250 mm × 4.6 mm; mobile phase, 1:1 CH_3CN:H_2O, 1 mL/min flow rate, RT = 7 min, 210−240 nm.

Brefeldin A 7-*O*-Methyl Glutarate (4). Brefeldin A 7-*O*-glutarate (**3**) (0.05 g, 0.13 mmol) was dissolved in methanol (2 mL) at room temperature. A 2 M solution of TMS diazomethane in hexane (0.2 mL, 0.4 mmol) was added. The reaction mixture was allowed to stir at room-temperature overnight. The progress of the reaction was monitored by silica gel TLC using 1:1 ethyl acetate−hexanes. More TMS diazomethane (0.25 mL, 0.56 mmol) was added after 24 h. After 48 h, the reaction was quenched by the addition of water (5 mL). The organic layer was washed with 0.1 M HCl (1 mL) and brine (2 × 1 mL) and dried over sodium sulfate. The solvent was evaporated, and the crude product was purified by flash chromatography on a silica gel column using a gradient eluant of 100% hexanes to 6:4 hexanes−ethyl acetate. Compound **4** was isolated as a white solid (0.065 g, 89%). Mp 84−85 °C. IR (thin film) 3469, 2929, 1711, 1258 cm^{-1}; ^{1}H NMR ($CDCl_3$, 300 MHz) δ 7.30 (dd, J = 3.13 and 15.70 Hz, 1 H), 5.90 (dd, J = 1.94 and 15.70 Hz, 1 H), 5.70 (m, 1 H), 5.15 (m, 1 H), 4.80 (m, 1 H), 4.12 (m, 1 H), 3.65 (s, 3 H), 2.10−2.40 (m, 9 H), 1.40−2.10 (m, 19 H), 1.25 (d, J = 6.21 Hz, 3 H), 0.90 (m, 1 H);

^{13}C NMR ($CDCl_3$, 300 MHz) δ 172.9, 151.7, 136.3, 131.4, 118.2, 76.2, 75.6, 72.1, 52.5, 52.0, 44.3, 40.5, 38.9, 34.5, 33.9, 33.5, 32.2, 27.0, 21.2, 20.6; ESIMS *m/z* 431 (Na^+ adduct). Anal. ($C_{22}H_{32}O_7$) C, H.

Brefeldin A 7-*O*-Glutarylamidohexanol (5). Compound **13** (0.06 g, 0.12 mmol) was dissolved in DMF (2 mL) at room temperature. TEA (0.02 mL, 0.16 mmol) was added to the solution. After 5 min of stirring, 6-aminohexanol (0.02 g, 0.16 mmol) was added to the solution. The reaction mixture was allowed to stir at room temperature for 16 h. The progress of the reaction was monitored by TLC using 10:1 chloroform−methanol. After 16 h, the reaction was quenched by the addition of water (5 mL). The aqueous layer was rinsed with dichloromethane (2 × 5 mL). The organic layer was washed with 0.5 M HCl (5 mL) and brine (5 mL) and dried over sodium sulfate. The crude product was purified by flash chromatography on silica gel using a gradient eluant of 100% hexanes to 7:3 ethyl acetate−hexanes. Compound **5** was isolated as a clear oil (0.026 g, 45%). IR (thin film) 3332, 2930, 2857, 1711, 1647, 1550, 1451, 1379, 1355, 1258, 1072, 756 cm^{-1}; ^{1}H NMR ($CDCl_3$, 300 MHz) δ 7.35 (dd, J = 3.07 and 15.66 Hz, 1 H), 5.90 (dd, J = 1.89 and 15.89 Hz, 1 H), 5.70 (m, 2 H), 5.15 (m, 2 H), 4.80 (m, 1 H), 4.12 (dt, J = 2.07 and 9.45 Hz, 1 H), 3.60 (t, J = 6.34 Hz, 2 H), 3.20 (q, J = 6.70 and 12.77 Hz, 2 H), 1.60−2.40 (m, 18 H), 1.20−1.60 (m, 9 H), 1.20 (d, J = 6.26 Hz, 3 H), 0.90 (m, 1 H); ^{13}C NMR ($CDCl_3$, 300 MHz) δ 173.9, 167.2, 153.2, 136.1, 131.2, 118.1, 75.5, 71.6, 62.0, 51.7, 40.3, 34.0, 27.1, 22.0, 20.5; ESIMS *m/z* 494 (MH^+); analytical LC: column, Microsorb Dynamax C1; column dimensions, 250 mm × 4.6 mm; mobile phase; 1:1 CH_3CN:H_2O, 1 mL/min flow rate, RT = 5.02 min, 230 nm.

Brefeldin A 4-*O*-Acetate (6). The title compound was isolated from the same crude mixture as that used for compound **2**. Compound **6** was a yellow oil (0.008 g, 7%). IR (thin film) 3457, 2936, 1741, 1708, 1449, 1380, 1230, 970 cm^{-1}; ^{1}H NMR ($CDCl_3$, 500 MHz) δ 7.15 (d, J = 15.77 Hz, 1 H), 5.65 (overlapping m and dd, 2 H), 5.20 (m, 2 H), 4.83 (m, 1 H), 4.10 (m, 1 H), 2.40 (m, 1 H), 1.40−2.20 (m, 9 H), 1.25 (d, J = 6.29 Hz, 3 H), 0.88−0.95 (m, 2 H); ^{13}C NMR ($CDCl_3$, 500 MHz) δ 170.0, 161.7, 140.3, 135.4, 118.2, 76.2, 75.6, 72.1, 49.5, 44.3, 43.2, 41.0, 40.5, 35.2, 31.9, 27.1, 26.2, 20.0; EIMS *m/z* 322 (M^+); analytical LC: column, Microsorb Dynamax C18; column dimensions, 250 × 4.6 mm; mobile phase, 1:1 CH_3CN-H_2O, 1 mL/min flow rate, RT = 8.33 min, 230 nm.

Brefeldin A 4-*O*-Glutarate (7). Brefeldin A 4-*O*-glutaryl 7-*O*-TBS silyl ether (**17**) (0.04 g, 0.09 mmol) was added to a round-bottomed flask containing 1 M TBAF in THF (0.30 mL, 0.30 mmol). The reaction mixture was stirred at 0 °C and slowly warmed to room temperature. The reaction progress was monitored by silica gel TLC using 6:4 hexanes−ethyl acetate with 2% acetic acid. The reaction was quenched after 25 h with 5% $NaHCO_3$ (10 mL) and extracted with dichloromethane (20 mL). The organic layer was washed with 1 M HCl (5 mL) and dried over sodium sulfate. Compound **7** was isolated as a yellow oil (0.026 g, 76%). IR (thin film) 3460, 2921, 2850, 1705, 1514, 1457, 1376, 1250, 748 cm^{-1}; ^{1}H NMR ($CDCl_3$, 300 MHz) δ 7.30 (dd, J = 3.41 and 13.02 Hz, 1 H), 5.65 (overlapping m and dd, 2 H), 5.30 (m, 2 H), 4.80 (m, 1 H), 4.20 (m, 1 H), 2.50 (m, 5 H), 2.10−2.25 (m, 2 H), 1.50−2.00 (m, 11 H), 1.25 (d, J = 6.25 Hz, 3 H), 0.80 (m, 1 H); ESIMS *m/z* 417 (Na^+ adduct); analytical LC: column, Microsorb Dynamax C18; column dimensions, 250 × 4.6 mm; mobile phase, 1:1 CH_3CN-H_2O, 1 mL/min flow rate, RT = 9.81 min, 230 nm.

Brefeldin A 4-*O*-Methyl Glutarate (8). Brefeldin A 4-*O*-methyl glutarate-7-*O*-TBS silyl ether (**18**) (0.036 g, 0.07 mmol) was dissolved in THF (0.8 mL) at 0 °C. A 1 M solution of TBAF in THF (0.13 mL, 0.13 mmol) was added dropwise over 45 min. The reaction mixture was allowed to warm to room temperature, and the progress of the reaction was monitored by silica gel TLC using 1:1 ethyl acetate−hexanes. After 48 h, the reaction was quenched by the addition of 5% $NaHCO_3$ (5 mL). The solution was extracted with dichloromethane (3 × 5 mL). The solvent was evaporated, and the crude product was purified by flash chromatography on silica gel using a gradient eluant of 100% hexanes to 6:4 hexanes−ethyl acetate. Compound **8** was isolated as an oil (0.012 g, 41%). IR (thin film) 3467, 2930, 1737, 1713, 1260 cm^{-1}; ^{1}H NMR ($CDCl_3$, 300 MHz) δ 7.20 (dd, J = 3.41 and 13.02 Hz, 1 H), 5.70 (overlapping m and dd, 2 H), 5.25 (overlapping m, 2 H), 4.80 (m, 1 H), 4.30 (m, 1 H), 3.65 (s, 3 H), 2.40 (m, 6 H), 2.10−2.25 (m, 2 H), 1.40−2.00 (m, 14 H), 1.25 (d, J = 6.25 Hz, 3 H), 0.90 (m, 1 H); ^{13}C NMR ($CDCl_3$, 300 MHz) δ 166.1, 147.7, 136.7, 131.1, 118.7, 76.8, 72.7, 72.3, 52.1, 49.9, 44.7, 43.6, 41.4, 34.5, 33.6, 33.4, 32.2, 27.0, 21.2, 20.5; ESIMS *m/z* 431 (Na^+ adduct); analytical LC: column, Microsorb Dynamax C18; column dimensions, 250 mm × 4.6 mm; mobile phase, 1:1 CH_3CN:H_2O, 1 mL/min flow rate, RT = 10.32 min, 230 nm.

Brefeldin A 4,7-*O*-Diacetate (9). The title compound was isolated from the same crude mixture as that used for compound **2**. Compound **9** was a white solid (0.009 g, 13%). Mp 122 °C. IR (thin film) 3488, 3019, 2930, 2400, 1708, 1648, 1215, 1133, 757 cm^{-1}; ^{1}H NMR ($CDCl_3$, 500 MHz) δ 7.20 (dd, J = 3.43 and 15.69 Hz, 1 H), 5.70 (overlapping m and dd, 2 H), 5.20 (overlapping m and dd, 2 H), 5.15 (m, 1 H), 4.80 (m, 1 H), 2.45 (m, 1 H), 2.30 (m, 1 H), 2.10 (s, 3 H), 2.00 (s, 3 H), 1.80 (m, 2 H), 1.60−1.75 (m, 2 H), 1.50−1.60 (m, 4 H), 1.25 (d, J = 6.29 Hz, 3 H), 0.88−0.95 (m, 2 H); ^{13}C NMR ($CDCl_3$, 300 MHz) δ 170.2, 169.9, 166.3, 147.2, 135.4, 131.0, 119.0, 76.3, 75.2, 49.3, 44.5, 40.1, 38.2, 31.6, 21.2, 20.8; EIMS *m/z* 364 (M^+). Anal. ($C_{20}H_{28}O_6$) C, H.

Brefeldin A 4,7-*O*-Diglutarate (10). Brefeldin A (0.10 g, 0.36 mmol) was added to a round-bottomed flask containing 2,6-lutidine (3 mL). Glutaric anhydride (0.21 g, 1.80 mmol) and DMAP (0.006 g, 0.05 mmol) were added to this solution. The mixture was allowed to stir at 110 °C for 24 h. The progress of the reaction was monitored by silica gel TLC using 7:3 ethyl acetate−hexanes with 1% acetic acid. The reaction was quenched with water (10 mL), and the mixture was extracted with dichloromethane (3 × 10 mL). The organic layer was washed with 1 M HCl (5 mL) and dried over sodium sulfate. Compound **10** was isolated as a clear oil (0.13 g, 71%). IR (thin film) 2933, 1711, 1410, 1379, 1260, 1162, 1075, 975, 914, 732 cm^{-1}; ^{1}H NMR ($CDCl_3$, 300 MHz) δ 7.23 (dd, J = 3.45 and 15.72 Hz, 1 H), 5.65 (overlapping m and dd, 2 H), 5.25 (m, 3 H), 4.85 (m, 1 H), 2.20−2.50 (m, 12 H), 1.50−2.10 (m, 16 H), 1.20 (d, J = 6.20 Hz, 6 H), 0.85 (m, 3 H); ^{13}C NMR ($CDCl_3$, 300 MHz) δ 179.0, 173.2, 172.9, 170.0, 166.3, 153.5, 136.2, 131.6, 75.6, 72.3, 50.8, 44.7, 40.6, 39.9, 34.5, 32.0, 30.5, 30.3, 26.8, 21.2; ESIMS *m/z* 531 (Na^+ adduct); analytical LC: column, Microsorb Dynamax C18; column dimensions, 250 mm × 4.6 mm; mobile phase, 1:1 CH_3CN:H_2O, 1 mL/min flow rate, RT = 8.60 min, 230 nm.

Brefeldin A 4,7-*O*-Di(methyl glutarate) (11). Brefeldin A (0.05 g, 0.18 mmol) was dissolved in dichloromethane (4 mL) at 0 °C. Triethylamine (0.05 mL, 0.36 mmol), 4-(dimethylamino)pyridine (0.004 g, 0.02 mmol), and methyl 5-chloro-5-oxovalerate (MCOV) (0.025 mL, 0.18 mmol) were added to the solution. The reaction mixture was allowed to warm to room temperature as it stirred overnight. The progress of the reaction was monitored by silica gel TLC using 1:1 ethyl acetate−hexanes. More MCOV (0.025 mL, 0.18 mmol) was added every 10 h until a total of 0.125 mL (0.9 mmol) had been added during the course of the reaction. After 48 h of reaction, dichloromethane (6 mL) was added to the reaction mixture. The organic layer was washed with 0.1 M HCl (1 mL) and brine (2 × 1 mL) and dried over sodium sulfate. Compound **11** was isolated as a clear oil (0.087 g, 91%). IR (thin film) 2952, 2932, 1738, 1733, 1715, 1438, 1258, 1200, 1174 cm^{-1}; ^{1}H NMR ($CDCl_3$, 300 MHz) δ 7.20 (dd, J = 3.45 and 15.72 Hz, 1 H), 5.65 (overlapping m and dd, 2 H), 5.25 (m, 3 H), 4.85 (m, 1 H), 3.65 (s, 3 H), 3.66 (s, 3 H), 2.20−2.50 (m, 12 H), 1.50−2.10 (m, 16 H), 1.20 (d, J = 6.20 Hz, 6 H), 0.85 (m, 3 H); ^{13}C NMR ($CDCl_3$, 300 MHz) δ 178.6, 173.8, 172.9, 172.2, 166.1, 147.5, 136.1, 131.6, 118.8, 76.6, 75.6, 72.3, 52.1, 50.1, 44.5, 40.5, 38.7, 34.5, 33.9, 33.4, 33.3, 32.1, 26.9, 21.1, 20.5, 20.2; ESIMS *m/z* 559 (Na^+ adduct). Anal. ($C_{28}H_{40}O_{10}$) C, H.

Brefeldin A 4,7-*O*-Di(glutarylamidohexanol) (12). Brefeldin A 4,7-*O*-diglutarate (**10**) (0.10 g, 0.2 mmol) was added to a round-bottomed flask containing dichloromethane (2 mL). 1-[3-(Di-

methylamino)propyl]-3-ethylcarbodiimide hydrochloride (EDCI) (0.10 g, 0.5 mmol) was added, and the mixture was allowed to stir at room temperature for 30 min. 6-Aminohexanol (0.06 g, 0.5 mmol) and triethylamine (0.05 mL, 0.36 mmol) were added to the solution, and the reaction was followed by silica gel TLC using 7:3 ethyl acetate−hexanes. After 4 h, the reaction had gone to completion as evidenced by the disappearance of the starting material. The reaction was quenched by the addition of water (10 mL). The organic layer was washed with water (5 × 5 mL) and dried by rotary evaporation. The crude product was purified by flash chromatography on silica gel using a gradient elution of 100% $CHCl_3$ to 1:1 $CHCl_3$−MeOH. Compound **12** was isolated as a yellow oil (0.015 g, 11%). IR (thin film) 3307, 2932, 2860, 1714, 1646, 1552, 1451, 1378, 1260, 1154, 1073, 1011, 798 cm^{-1}; ^1H NMR ($CDCl_3$, 300 MHz) δ 7.20 (dd, J = 3.49 and 15.78 Hz, 1 H), 5.65 (overlapping m and dd, 2 H), 5.25 (m, 3 H), 4.85 (m, 1 H), 3.60 (t, J = 6.26 Hz, 4 H), 3.66 (s, 3 H), 3.25 (br s, 5 H), 2.80 (br s, 5 H), 2.20−2.50 (m, 13 H), 1.60−2.10 (m, 15 H), 1.55 (m, 12 H), 1.35 (m, 11 H), 1.20 (d, J = 6.25 Hz, 4 H), 0.90 (m, 1 H); ^{13}C NMR ($CDCl_3$, 300 MHz) δ 173.8, 172.9, 172.2, 166.1, 147.5, 136.1, 132.0, 118.4, 75.3, 72.3, 50.1, 44.8, 40.7, 38.3, 35.5, 33.9, 33.4, 33.1, 32.1, 30.2, 27.0, 25.6, 21.4, 20.2; ESIMS m/z 729 (Na^+ adduct); analytical LC: column, Microsorb Dynamax C18; column dimensions, 250 mm × 4.6 mm; mobile phase, 1:1 CH_3CN:H_2O, 1 mL/min flow rate, RT = 5.47 min, 230 nm.

Brefeldin A 7-*O*-Glutaryl-*N*-hydroxysuccinimidyl Ester (13). Compound **3** (0.07 g, 0.17 mmol) was dissolved in DMF (3 mL) and 2,6-lutidine (0.50 mL). The solution was stirred at 60 °C for 5 min. *N*,*N*′-Disuccinimidyl carbonate (0.054 g, 0.2 mmol) was added and the mixture stirred overnight at 60 °C. The progress of the reaction was monitored by silica gel TLC using 7:3 ethyl acetate−hexanes. After 24 h, more *N*,*N*′-disuccinimidyl carbonate (0.03 g, 0.12 mmol) was added and the reaction mixture stirred for another 24 h. The crude mixture was purified by column chromatography on silica gel using a gradient elution of 100% hexanes to 100% ethyl acetate. Product **13** was isolated as a clear oil (0.028 g, 48%). IR (thin film) 3490, 2933, 1814, 1785, 1739, 1451, 1360, 1256, 1206, 1070, 984, 915, 732, 648 cm^{-1}; ^1H NMR ($CDCl_3$, 300 MHz) δ 7.35 (dd, J = 3.10 and 15.68 Hz, 1 H), 5.90 (dd, J = 1.89 and 15.69 Hz, 1 H), 5.70 (m, 1 H), 5.20 (m, 2 H), 4.80 (m, 1 H), 4.20 (m, 2 H), 2.20−2.50 (m, 8 H), 1.40−2.10 (m, 11 H), 1.20 (m, 4 H), 0.09 (m, 2 H); ^{13}C NMR ($CDCl_3$, 300 MHz) δ 173.0, 171.0, 169.6, 166.0, 152.2, 143.0, 136.2, 119.0, 76.2, 72.1, 52.4, 44.3, 33.2, 26.0, 20.2; ESIMS m/z 492 (MH^+).

Brefeldin A 7-*O*-TBS Silyl Ether (14). Brefeldin A (0.20 g, 0.71 mmol) was added to a round-bottomed flask containing dichloromethane (0.7 mL) at 0 °C. 2,6-Lutidine (86 μL) was added to this solution. TBSOTf (0.25 mL, 1.0 mmol) was added dropwise to the reaction mixture, which was allowed to warm to room temperature and stir for 8 h. The progress of the reaction was monitored by silica gel TLC using 8:2 hexanes−ethyl acetate. The reaction was quenched by the addition of a 5% $NaHCO_3$ solution (2 mL). The mixture was extracted with dichloromethane (3 × 15 mL) and then dried over Na_2SO_4. The solvent was evaporated, and the crude product was purified by flash chromatography on silica gel using a gradient eluant of 100% hexane to 8:2 hexanes−ethyl acetate. The disilylated, 7-silylated, and 4-silylated compounds were obtained in 40, 22, and 4% yields, respectively. Compound **14** was isolated as a thick clear oil (0.062 g, 22%). We also found that when compound **16** (0.100 g, 0.2 mmol) was deprotected by the addition of 1 M TBAF in THF (0.100 mL, 0.1 mmol) dropwise over 2 h the 7-silylated compound was the only product isolated in 64% yield. This was combined with the previously isolated BFA 7-*O*-TBS silyl ether **14**. Such selective desilylations of allylic silyl ethers have been previously reported.[39,40] IR (thin film) 3441, 2929, 1715, 1254, 1122, 968, 913, 775, 735 cm^{-1}; ^1H NMR ($CDCl_3$, 300 MHz) δ 7.27 (dd, J = 3.25 and 13.91 Hz, 1 H), 5.85 (dd, J = 1.79 and 15.50 Hz, 1 H), 5.60 (m, 1 H), 5.25 (m, 1 H), 4.82 (m, 1 H), 4.20 (p, J = 4.84 Hz, 1 H), 4.05 (m, 1 H), 2.25 (m, 1 H), 1.60−2.0 (m, 10 H), 1.50 (m, 2 H), 1.25 (d, J = 6.25 Hz, 3 H), 0.85 (s, 9 H), 0.021 (s, 3 H), 0.017 (s, 3 H); ^{13}C NMR ($CDCl_3$, 300 MHz) δ 166.7, 152.2, 137.3, 130.4, 117.8, 76.5, 73.3, 72.2, 52.5, 44.5, 43.9, 41.7, 34.5, 32.3, 27.2, 26.3, 21.3, 19.5, −4.4; ESIMS m/z 417 (Na^+ adduct).

Brefeldin A 4-*O*-TBS Silyl Ether (15). This analogue was isolated from the same reaction mixture as that used for compound **14**. Compound **15** was obtained as a clear oil (0.011 g, 4%). ^1H NMR ($CDCl_3$, 300 MHz) δ 7.30 (dd, J = 3.19 and 15.46 Hz, 1 H), 5.85 (dd, J = 1.79 and 15.50 Hz, 1 H), 5.60 (m, 1 H), 5.25 (m, 1 H), 4.85 (m, 1 H), 4.20 (p, J = 4.93 Hz, 1 H), 4.05 (dt, J = 2.97 and 9.00 Hz, 1 H), 2.10−2.30 (m, 2 H), 1.90−2.00 (m, 3 H), 1.30−1.90 (m, 8 H), 1.25 (d, J = 6.28 Hz, 4 H), 0.90 (s, 9 H), 0.47 (s, 3 H), −0.0039 (s, 3 H).

Brefeldin A 4,7-*O*-TBS Disilyl Ether (16). This analogue was isolated from the same reaction mixture as that used for compound **14**. Compound **16** was obtained as a clear oil (0.145 g, 40%). ^1H NMR ($CDCl_3$, 300 MHz) δ 7.30 (dd, J = 3.06 and 15.57 Hz, 1 H), 5.85 (dd, J = 1.73 and 15.51 Hz, 1 H), 5.60 (m, 1 H), 5.25 (m, 1 H), 4.85 (m, 1 H), 4.20 (p, J = 4.59 Hz, 1 H), 4.05 (d, J = 8.68 Hz, 1 H), 2.10−2.30 (m, 2 H), 1.60−2.00 (m, 8 H), 1.5 (m, 3 H), 1.25 (d, J = 6.26 Hz, 4 H), 0.95 (s, 9 H), 0.85 (s, 9 H), 0.034 (s, 3 H), 0.016 (s, 3 H), 0.010, (s, 3 H), −0.0064 (s, 3 H); ^{13}C NMR ($CDCl_3$, 300 MHz) δ 166.8, 152.9, 137.7, 129.7, 118.4, 73.2, 71.8, 53.2, 44.2, 42.4, 34.5, 32.3, 27.1, 26.3, 21.3, 18.5, −3.7, −4.4; CIMS m/z 509 (MH^+). Anal. ($C_{28}H_{52}O_4Si_2$) C, H.

Brefeldin A 4-*O*-Glutaryl 7-*O*-TBS Silyl Ether (17). Brefeldin A 7-*O*-TBS silyl ether (**14**) (0.04 g, 0.10 mmol) was added to a round-bottomed flask containing 2,6-lutidine (1 mL). Glutaric anhydride (0.03 g, 0.30 mmol) was added to the solution. DMAP (0.006 g, 0.05 mmol) was added to the reaction mixture. The mixture was allowed to stir at 110 °C overnight. The progress of the reaction was monitored by silica gel TLC using 8:2 hexanes−ethyl acetate and 1% acetic acid. The reaction was quenched with water (5 mL), and the mixture was extracted with dichloromethane (4 × 5 mL). The organic layer was washed with 1 M HCl (5 mL) and dried over sodium sulfate. The solvent was evaporated, and the crude product was purified by column chromatography on a silica gel column eluted using a gradient of 100% hexanes to 1:1 hexanes−ethyl acetate. Compound **17** was isolated as a yellow oil (0.044 g, 87%). ^1H NMR ($CDCl_3$, 300 MHz) δ 7.30 (dd, J = 3.82 and 15.52 Hz, 1 H), 5.65 (overlapping m and dd, 2 H), 5.30 (m, 2 H), 4.80 (m, 1 H), 4.20 (m, 1 H), 2.70 (t, J = 6.65 Hz, 1 H), 2.30−2.50 (m, 6 H), 1.80−2.10 (m, 6 H), 1.60−1.80 (m, 5 H), 1.50 (m, 4 H), 1.20 (d, J = 6.25 Hz, 4 H), 0.80 (overlapping s and m 10 H), 0.00 (m, 10 H); ^{13}C NMR ($CDCl_3$, 300 MHz) δ 172.3, 147.9, 137.1, 130.6, 118.5, 73.2, 72.3, 49.9, 43.9, 41.6, 34.5, 33.5, 33.2, 27.1, 26.2, 21.2, 20.2, −4.4.

Brefeldin A 4-*O*-Methyl Glutarate-7-*O*-TBS Silyl Ether (18). Brefeldin A 4-*O*-glutarate-7-*O*-TBS silyl ether (**17**) (0.05 g, 0.09 mmol) was dissolved in methanol (1 mL) at room temperature. A 2 M solution of TMS diazomethane in hexane (0.14 mL, 0.28 mmol) was dissolved in hexane (0.14 mL, 0.28 mmol) and added to the solution. The reaction mixture was allowed to stir at room temperature, and the progress of the reaction was monitored by silica gel TLC using 1:1 ethyl acetate−hexanes. More TMS diazomethane was added to the reaction mixture every 12 h, until a total of 0.70 mL (1.5 mmol) was added during the entire course of the reaction. After 48 h, the reaction mixture was washed with brine (10 mL) and dried over sodium sulfate. Compound **18** was isolated as a yellow oil (0.036 g, 75%). IR (thin film) 2953, 2930, 1741, 1717, 1256 cm^{-1}; ^1H NMR ($CDCl_3$, 300 MHz) δ 7.30 (dd, J = 3.32 and 15.63 Hz, 1 H), 5.65 (overlapping m and dd, 2 H), 5.20 (overlapping m, 2 H), 4.80 (m, 1 H), 4.20 (t, J = 4.15 Hz, 1 H), 3.65 (s, 3 H), 2.40 (m, 5 H), 1.60−2.10 (m, 12 H), 1.50 (m, 4 H), 1.20 (d, J = 6.29 Hz, 5 H), 0.90 (s, 11 H), 0.00 (s, 7 H); ^{13}C NMR ($CDCl_3$, 300 MHz) δ 173.6, 172.9, 166.1, 147.9, 137.0, 130.6, 118.5, 73.2, 72.3, 52.1, 49.9, 44.6, 43.9, 41.6, 34.4, 33.6, 33.4, 30.1, 27.0, 26.2, 21.2, 20.5, 18.4, −4.4.

Metabolic Stabilities of BFA Analogues. The analogues were incubated with rat plasma at 37 °C for varying time periods, and the degradation of the compounds was monitored by HPLC.[41] The analogues and salicylic acid (internal standard) were dissolved in

methanol (1 mL) at concentrations of 17.8 and 10 mM, respectively. This stock solution was filtered through a 0.45 μM filter. Lyophilized rat plasma (Lot 052K7609, Sigma) was reconstituted in water (1.0 mL). This plasma solution was heated at 37 °C for 15 min. A 0.01 M solution of phosphate buffered saline (PBS) (0.25 mL, pH 7.0) was added to afford an 80% plasma solution. The solution was incubated for 5 min at 37 °C. The stock solution (100 μL) was added to the rat plasma solution, and the final concentrations of drug and internal standard were 1.4 and 0.8 mM, respectively. The solution was allowed to incubate at 37 °C, and aliquots were removed at various time points. Hydrolysis was quenched by the addition of acetonitrile (90 μL), which precipitated the protein. The samples were centrifuged at 14 000 rpm for 5 min, and the supernatant (20 μL) was injected into an HPLC column for analysis. The HPLC system was a Beckman 125 solvent delivery module with a 166 detector set at 230 nm. The mobile phase was 57:43 methanol−water with 0.1% TFA. The flow rate was 1 mL/min and the stationary phase was a Dynamax Microsorb C18 column (250 mm × 4 mm). The results of this analysis are given in Table 2.

Molecular Modeling. The crystal structure of BFA in the interface between ARF1-GDP and its GEF protein ARNO was downloaded from the Protein Data Bank (PDB code 1R8Q).[18] The structure of BFA 7-*O*-methyl glutarate was constructed in Sybyl v. 7.0 and overlapped with the structure of BFA in the binding pocket, and BFA was then deleted. The MMFF94s force field with MMFF94 charges were used to minimize the energy of the new complex. The energy minimization was performed using the Powell method with a 0.05 kcal/mol·Å gradient convergence criterion and a distance-dependent dielectric constant. During the minimization, the structures of the analogue, protein, and nucleotide were allowed to move. BFA 4-*O*-methyl glutarate (**8**) and BFA 7-*O*-glutaryl-amidohexanol (**5**) were also modeled into this binding site in a similar fashion (Figure 3).

Confocal Microscopy. HCT116 cells were grown on Labtek coverglass plates to 60−70% confluency and treated with 0.3 μM BFA (**1**) or analogues **4**, **8**, or **10** for 45 min at 37 °C. The growth media were removed, and the cells were washed with PBS to remove the excess drug. The cells were fixed in a formaldehyde solution (4%) for 10 min at 37 °C, after which the formaldehyde was removed, and the cells were rinsed with PBS. The NBD ceramide−BSA conjugate stock solution was prepared by dissolving NBD ceramide (Molecular Probes) (1 mg) in a solution of bovine serum albumin (0.68 mg) in McCoy's 5A medium (1 mL). The cells were then incubated in fresh media containing 10 μM NBD ceramide−BSA conjugate for 10 min at 37 °C. The cells were washed again to remove the excess dye before the cells were visualized by confocal microscopy using the Bio-Rad MRC1024 inverted microscope at the Purdue University Cytometry Lab. The images in Figure 4 show the ability of the BFA analogues to disrupt the Golgi complex compared to that of the parent compound.

Acknowledgment. We would like to thank the UNCF-Merck Science Initiative, and the Purdue University Cancer Center for their support of this research. We also thank the Developmental Therapeutics Program, NIH for generously donating brefeldin A.

Supporting Information Available: Results of the experimental HPLC analyses and elemental analyses. This material is available free of charge via the Internet at http://pubs.acs.org.

References

(1) Singleton, V. L.; Bohonos, N.; Ullstrupp, A. J. Decumbin, a New Compound from a Species of *Penicillium*. *Nature* **1958**, *181*, 1072−1073.

(2) Fox, B. M.; Vroman, J. A.; Fanwick, P. E.; Cushman, M. Preparation and Evaluation of Sulfide Derivatives of the Antibiotic Brefeldin A as Potential Prodrug Candidates with Enhanced Aqueous Solubilities. *J. Med. Chem.* **2001**, *44*, 3915−3924.

(3) Argade, A. B.; Devraj, R.; Vroman, J. A.; Haugwitz, R. D.; Hollingshead, M.; Cushman, M. Design and Synthesis of Brefeldin A Sulfide Derivatives as Prodrug Candidates with Enhanced Aqueous Solubiities. *J. Med. Chem.* **1998**, *41*, 3337−3346.

(4) Argade, A.; Haugwitz, R. D.; Devraj, R.; Cushman, M. Highly Efficient Diastereoselective Michael Addition of Various Thiols to (+)-Brefeldin A. *J. Org. Chem.* **1998**, *63*, 273−278.

(5) Takatsuki, A.; Yamaguchi, I.; Tamura, G.; Misato, T.; Arima, K. Antiviral and Antitumor Antibiotics. XIX. Correlation between the Antianimal- and Antiplant-virus Activities of Several Antibiotics. *J. Antibiot.* **1969**, *22*, 442−445.

(6) Kikuchi, S.; Shinpo, K.; Tsuji, S.; Yabe, I.; Niino, M.; Tashiro, K. Brefeldin A-Induced Neurotoxicity in Cultured Spinal Cord Neurons. *J. Neurosci. Res.* **2003**, *71*, 591−599.

(7) Dinter, A.; Berger, E. G. Golgi-disturbing Agents. *Histochem. Cell Biol.* **1998**, *109*, 571−590.

(8) Fujiwara, T.; Oda, K.; Yokota, S.; Takatsuki, A.; Ikehara, Y. Brefeldin A Causes Disassembly of the Golgi Complex and Accumulation of Secretory Proteins in the Endoplasmic Reticulum. *J. Biol. Chem.* **1988**, *263*, 18545−18552.

(9) Driouich, A.; Zhang, G. F.; Staehelin, L. A. Effect of Brefeldin A On the Structure of the Golgi Apparatus and on the Synthesis and Secretion of Proteins and Polysaccharides in Sycamore Maple (*Acer pseudoplatanus)* Suspension-Cultured Cells. *Plant Physiol.* **1993**, *101*, 1363−1373.

(10) Lippincott-Schwartz, J.; Yuan, L. C.; Bonifacino, J. S.; Klausner, R. D. Rapid Redistribution of Golgi Proteins Into the ER in Cells Treated with Brefeldin A: Evidence for Membrane Cycling from Golgi to ER. *Cell* **1989**, *56*, 801−813.

(11) Donaldson, J. G.; Cassel, D.; Kahn, R. A.; Klausner, R. D. ADP-Ribosylation Factor, a Small GTP-Binding Protein, Is Required for Binding of the Coatomer Protein Beta-COP to Golgi Membranes. *Proc. Natl. Acad. Sci. U.S.A.* **1992**, *89*, 6408−6412.

(12) Donaldson, J. G.; Kahn, R. A.; Lippincott-Schwartz; Klausner, R. D. Binding of ARF and Beta-COP to Golgi Membranes: Possible Regulation by a Trimeric G Protein. *Science* **1991**, *254*, 1197−1199.

(13) Donaldson, J. G.; Jackson, C. L. Regulators and Effectors of the ARF GTPases. *Curr. Opin. Cell Biol.* **2000**, *12*, 475−482.

(14) Cockcroft, S.; Thomas, G. M.; Fensome, A.; Geny, B.; Cunningham, E.; Gout, I.; Hiles, I.; Totty, N. F.; Truong, O.; Hsuan, J. J. Phospholipase D: a Downstream Effector of ARF in Granulocytes. *Science* **1991**, *263*, 523−526.

(15) Cockcroft, S. Signaling Roles of Mammalian Phospholipase D1 and D2. *Cell. Mol. Life Sci.* **2001**, *58*, 1674−1687.

(16) Cockcroft, S. ARF−Regulated Phospholipase D: a Potential Role in Membrane Traffic. *Chem. Phys. Lipids* **1996**, *80*, 59−80.

(17) Robineau, S.; Chabre, M.; Antonny, B. Binding Site of Brefeldin A at the Interface Between the Small G-Protein ADP Ribosylation Factor 1 (ARF1) and the Nucleotide Exchange Factor Sec7 Domain. *Proc. Natl. Acad. Sci. U.S.A.* **2000**, *97*, 9913−9918.

(18) Renault, L.; Guibert, B.; Cherfils, J. Structural Snapshots of the Mechanism and Inhibition of a Guanine Nucleotide Exchange Factor. *Nature* **2003**, *426*, 525−530.

(19) Cherfils, J.; Menetrey, J.; Mathieu, M.; La Bras, G.; Robineau, S.; Beraud-Dufour, S.; Antonny, B.; Chardin, P. Structure of the Sec7 Domain of the Arf Exchange Factor ARNO. *Nature* **1998**, *392*, 101−105.

(20) Goldberg, J. Structural Basis for Activation of ARF GTPase: Mechanisms of Guanine Nucleotide Exchange and GTP-Myristoyl Switching. *Cell* **1998**, *95*, 237−248.

(21) Sata, M.; Moss, J.; Vaughan, M. Structural Basis for the Inhibitory Effect of Brefeldin A on Guanine Nucleotide-Exchange Proteins for ADP-Ribosylation Factors. *Proc. Natl. Acad. Sci. U.S.A.* **1999**, *96*, 2752−2757.

(22) Mossessova, E.; Corpina, R. A.; Goldberg, J. Crystal Structure of ARF1·Sec7 Complexed with Brefeldin A and Its Implications for the Guanine Nucleotide Exchange Mechanism. *Mol. Cell* **2003**, *12*, 1403−1411.

(23) Lippincott-Schwartz, J.; Glickman, J.; Donaldson, J. G.; Robbins, J.; Kreis, T. E.; Seamon, K. B.; Sheetz, M. P.; Klausner, R. D. Forskolin Inhibits and Reverses the Effects of Brefeldin-a on Golgi Morphology by a Camp-Independent Mechanism. *J. Cell Biol.* **1991**, *112*, 567−577.

(24) Nojiri, H.; Manya, H.; Isono, H.; Yamana, H.; Nojima, S. Induction of Terminal Differentiation and Apoptosis in Human Colonic Carcinoma Cells by Brefeldin A, a Drug Affecting Ganglioside Biosynthesis. *FEBS Lett.* **1999**, *453*, 140−144.

(25) Zhu, J. W.; Nagasawa, H.; Nagura, F.; Mohamad, S. B.; Uto, Y.; Ohkura, K.; Hori, H. Elucidation of Strict Structural Requirements of Brefeldin A as an Inducer of Differentiation and Apoptosis. *Bioorg. Med. Chem.* **2000**, *8*, 455−463.

(26) Zhu, J.-W.; Hori, H.; Nojiri, H.; Tsukuda, T.; Taira, Z. Synthesis and Activity Of Brefeldin A Analogs as Inducers of Cancer Cell Differentiation and Apoptosis. *Bioorg. Med. Chem. Lett.* **1997**, *7*, 139−144.
(27) Wu, Y. K.; Shen, X.; Yang, Y. Q.; Hu, Q.; Huang, J. H. Enantioselective Total Synthesis of (+)-Brefeldin A and 7-*epi*-Brefeldin A. *J. Org. Chem.* **2004**, *69*, 3857−3865.
(28) Gorst-Allman, C. P.; Steyn, P. S.; Rabie, C. J. 7-*epi*-Brefeldin A, a Co-Metabolite of Brefeldin A in *Curvularia lunata*. *J. Chem. Soc., Perkin Trans. 1* **1982**, 2387−2390.
(29) Proksa, B.; Uhrin, D.; Adamcova, J.; Fuska, J. Oxidation of Brefeldin A. *Pharmazie* **1992**, *47*, 582−584.
(30) Helms, J. B.; Rothman, J. E. Inhibition by Brefeldin A of a Golgi Membrane Enzyme That Catalyzes Exchange of Guanine-Nucleotide Bound to ARF. *Nature* **1992**, *360*, 352−354.
(31) Corey, E. J.; Cho, H.; Rucker, C.; Hua, D. H. Studies with Trialkylsilyltriflates − New Syntheses and Applications. *Tetrahedron Lett.* **1981**, *22*, 3455−3458.
(32) Corey, E. J.; Venkateswarlu, A. Protection of Hydroxyl Groups as *tert*-Butyldimethylsilyl Derivatives. *J. Am. Chem. Soc.* **1972**, *94*, 6190−6191.
(33) Park, Y.; Albright, K. J.; Cai, Z. Y.; Pariza, M. W. Comparison of Methylation Procedures for Conjugated Linoleic Acid and Artifact Formation by Commercial (Trimethylsilyl)diazomethane. *J. Agric. Food Chem.* **2001**, *49*, 1158−1164.
(34) Jacobi, P. A.; Li, Y. K. Enantioselective Syntheses of Ring-C Precursors of Vit. B-12. Reagent Control. *Org. Lett.* **2003**, *5*, 701−704.
(35) Morpurgo, M.; Bayer, E. A.; Wilchek, M. *N*-Hydroxysuccinimide Carbonates and Carbamates are Useful Reactive Reagents for Coupling Ligands to Lysines on Proteins. *J. Biochem. Biophys. Methods* **1999**, *38*, 17−28.
(36) Phillips, L. R.; Supko, J. G.; Malspeis, L. Analysis of Brefeldin A in Plasma by Gas Chromatography with Electron Capture Detection. *Anal. Biochem.* **1993**, *211*, 16−22.
(37) Phillips, L. R.; Wolfe, T. L.; Malspeis, L.; Supko, J. G. Analysis of Brefeldin A and the Prodrug Breflate in Plasma by Gas Chromatography with Mass Selective Detection. *J. Pharm. Biomed. Anal.* **1998**, *16*, 1301−1309.
(38) Brüning, A.; Ishikawa, T.; Kneusel, E.; Matern, U.; Lottspeich, F.; Wieland, F. T. Brefeldin A Binds to Glutathione *S*-Transferase and Is Secreted as Glutathione and Cysteine Conjugates by Chinese Hamster Ovary Cells. *J. Biol. Chem.* **1992**, *267*, 7726−7732.
(39) Charest, M. G.; Lerner, C. D.; Brubaker, J. D.; Siege, D. R.; Myers, A. G. A Convergent Enantioselective Route to Structurally Diverse 6-Deoxytetracycline Antibiotics. *Science* **2005**, *308*, 395−398.
(40) Sinha, S. C.; Barbas, C. F.; Lerner, R. A. The Antibody Catalysis Route to the Total Synthesis of Epothilones. *Proc. Natl. Acad. Sci. U.S.A.* **1998**, *95*, 14603−14608.
(41) Silvestri, M. A.; Nagarajan, M.; De Clercq, E.; Pannecouque, C.; Cushman, M. Design, Synthesis, Anti-HIV Activities, and Metabolic Stabilities of Alkenyldiarylmethane (ADAM) Non-Nucleoside Reverse Transcriptase Inhibitors. *J. Med. Chem.* **2004**, *47*, 3149−3162.

JM0602817